Implementing Inertial Measurement Unit on Covid Robot with Complementary and Madgwick Filter

Arjon Turnip, Muhammad Iqbal Fadlillah and Erwin Sitompul

***Abstract*— Rapidly developing technology causes autonomous robots to develop significantly as well. This causes the demand for autonomous robots to increase in various industrial sectors ranging from agriculture, large-scale manufacturing industries, and even hospitals. Especially in the midst of the Covid-19 pandemic where physical distancing is applied to make autonomous robots that can be used as a substitute for medical personnel. The Inertial Measurement Unit (IMU) is a very important part of an autonomous robot because the IMU can measure 3 axes. The IMU sensor has been integrated with 3 other sensors, namely accelerometer, gyroscope, and magnetometer sensors. However, the data obtained from the sensor has an error value that can cause noise. Therefore, a filter is needed to get high accuracy results. In this study, complementary methods and Madgwick filters were used to reduce noise in the raw data so that the results can be maximized.**

***Index Terms* — Robot Autonomous, Covid-19, Inertial Measurement Unit (IMU), Complementary Filter, Madgwick Filter.**

I. INTRODUCTION

AUTOMATION has now entered all aspects of human life, one of which is in the health sector. This is due to the Covid-19 pandemic which demands the application of physical distancing so that robot technology autonomous can be utilized [1], [2]. The rapid development of robots every year causes the development of robot research to autonomous to begin to develop after the 20th century [3]. This is supported by the demand for technology Robot Process Automation rapidly increasing (RPA)and it is estimated that up to 90% of industries use RPA by 2020 [4]. Robots Autonomous requires learning of the navigation system so that the robot can move in all directions properly [5].

The problem that will be faced by robots autonomous is that when the robot is moving automatically towards its destination, the robot has many obstacles. The navigation error will increase over time due to the integration of measurements noise [6]. To overcome these problems, autonomous robots must be added with sensors that can detect these navigational errors. In autonomous robots, obstacle avoidance can distinguish obstacles from transmittable areas to make decisions about their navigation [7]. The component that can be used to solve this problem is the Inertial Measurement Unit (IMU). The robot navigation system requires assistance from the IMU sensor to determine the robot's orientation when doing localization. The implementation of the IMU on the covid robot serves to determine the tilt of the robot, the acceleration of the robot, and the robot's magnetic field with respect to the earth. IMU is a physical sensor to help determine the estimated location and location of the robot [8]. In addition, IMU cooperates with LiDAR to assist the robot's work during mapping [9].

IMU consists of 2 types, namely 6-DOF and 9-DOF both have 3 types of sensors, namely, accelerometer, gyroscope, and magnetometer [10]. Each sensor has 3 different values based on its reference axis, namely the x-axis, (roll axis), y-axis (pitch axis), and z-axis (yaw axis) [11]. The IMU sensor has a bias value that causes the resulting output to have value drift (error) so a filter is needed to reduce the value error. There are several filter methods that can be used, including Kalman Filter, Mahony, Madgwick, Geometric Stochastic, Complementary Filter, Extended Kalman Filter (EKF), Unscented Kalman Filter (UKF) [12]–[17]. In this study, two methods were used, namely Complementary and Madgwick Filter.

A complementary filter is a filter method with a less complex application because it does not require many variables, only a few variables such as alpha (filter coefficient), sampling time, slope values gyroscope, and accelerometer. While the Madgwick Filter is the development of a more efficient Mahony filter. Madgwick Filter has the advantage that it does not require a lot of memory, is effective at low-sampling rates (10 Hz) and has better accuracy than the Kalman Filter [18]. There are many studies and applications of IMU sensors such as motion trajectory tracking in geodetic survey applications [19], mobile robot positioning with 2 sensors [20], navigation indoor [21], autonomous underwater vehicles [22], the use of IMU and LiDAR in an indoor environment. room [9]. The purpose of this study was to determine the best filter to be used in the implementation of the IMU on the covid robot.

II. METHODOLOGY

In the covid robot research, this research has used LiDAR 3D and LiDAR 2D mapping sensors as navigation and rotary encoder as speed sensors and position sensors. These two sensors play an important role in the navigation of the COVID-

Arjon Turnip and Muhammad Iqbal Fadlillah. Department of Electrical Engineering, Universitas Padjadjaran, Indonesia. (e-mail: turnip@unpad.ac.id*).

Erwin Sitompul. Study Program of Electrial Engineering, President University, Indonesia. (email:sitompul@president.ac.id)

19 autonomous robot. In order to integrate LiDAR and the rotary encoder, an IMU sensor is needed, the sensor Inertial Measurement Unit will be installed on this covid robot to get a better and more accurate navigation path. All sensors contained in the robot will be processed using Intel NUC as the robot control center. This paper focuses on collecting IMU sensor data to estimate the robot's accuracy when navigating by eliminating the noise generated by the IMU sensor. Data collection will be carried out in the Universitas Padjadjaran Test Room. The following is the composition of the Covid robot components and the data collection locations are shown in Fig. 1.

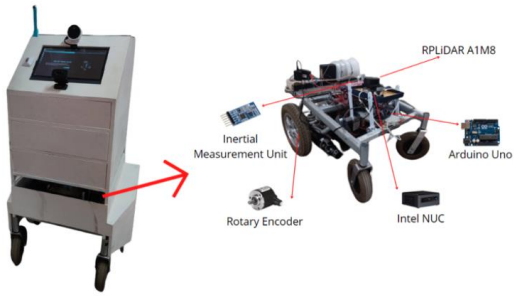

(a)

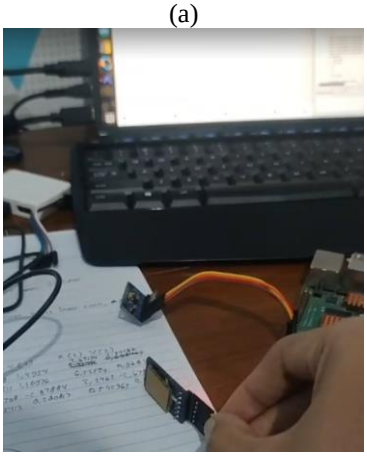

(b)

Fig 1. (a) The composition of the Robot Covid, (b) Data collection location

The IMU sensor has a value error generated by the IMU sensor itself, if it is integrated over time, the error value will be even greater. Therefore, a filter is needed to overcome this. The method used to filter the IMU sensor in this study is the Robot Operating System (ROS) Complementary and the algorithm Madgwick filter. Complementary filters use a combination of sensors accelerometer and gyroscope to perform the filter. The sensor is accelerometer values, long-term while the gyroscope is used to take used to retrieve data short-term. The two things are put together through mathematical calculations, the value of the will be obtained complementary filter. In Inertial Measuring Units (IMU), there are two methods to calculate the angle of position of the robot. One such method for calculating angles is to integrate the angular velocity of gyroscopes using the formula in equation (1). The first equation is the process of converting the output value obtained from gyroscope sensor into an angle value with degree units. The unit value obtained from the initial angle (in degrees) is then added with integral results of angular velocity in the time range from 0 until t which is read in the gyroscope sensor.

$$angle_{\Omega y} = angle_0 + \int_0^t \Omega y \, dt, \quad (1)$$

where the angle Ω is the initial angle of the object's position. Meanwhile, angle y is the calculated value obtained from the angular velocity of the gyroscopes. This keeps can also be related to the acceleration of three axes in the coordinate system by using an accelerometer, where the accelerometer is a sensor used to measure the speed of an object. In the calculation below, the accelerometer can calculate the roll and pitch angles.

$$\begin{cases} \Phi = \arctan\frac{a_y}{a_z} \ (-\pi, \pi) \\ \theta = \arcsin -\frac{a_y}{g} \ (-\frac{\pi}{2}, \frac{\pi}{2}) \\ \varphi = \arctan\frac{m_x}{m_y} \ (-\pi, \pi) \end{cases} \quad (2)$$

The equation (2) is the calculation of the accelerometer sensor and magnetometer on the IMU. Where x, y, and z is the value of the three axes obtained after applying accelerometer calibration in the raw data measurements (ax, ay, and az). Meanwhile, g is the vector of gravitational velocity that perpendicular to the ax and az value. The values of mx and my are the magnetic induction intensity of the system. Roll is the rotation between the front to the back of the axis, while the pitch is the side-to-side rotation of the axle. This calculation also uses a magnetometer to calculate the yaw angle, where the yaw angle is the rotation between the vertical angles. From the two formulas above, after being implemented the use of an accelerometer has static stability, but is susceptible to high-frequency signals and is less reliable to vibration. Meanwhile, the use of gyroscopes has better dynamic stability, while the data is relatively unreliable in a stable environment. According to sources [21]-[25], filter algorithms complementary can combine the two sensors above to correct integration errors with gyroscopes and rely on stability with accelerometers. The following block diagram of the Complementary filter is shown in Fig. 2.

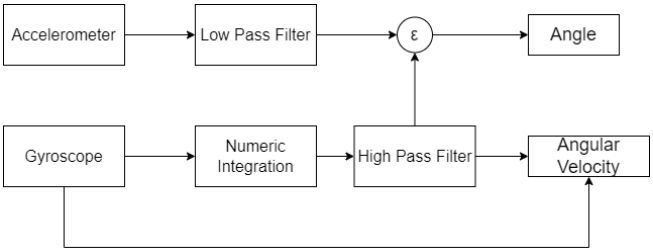

Fig 2. Complementary filter block diagram.

In the Madgwick filter, there are several filter stages, namely Orientation from angular rate, Orientation from vector observations, Filter fusion algorithm, Magnetic distortion compensation, Gyroscope bias drift compensation, and Filter gains. Some of these stages will form the optimal movement output for the robot. In the Orientation from the angular rate stage, the 3-axis gyroscope will process the input x, y, and z by measuring the speed. Then at the Orientation from the vector observations stage the data obtained will be processed by measuring the magnitude and direction of the gravitational field. But when measuring the magnitude and direction of the gravitational field there is a disturbance from the linear acceleration due to the sensor moving continuously.

Furthermore, at the filter fusion algorithm stage, it will process the data on the previous filter where the output of the filter fusion algorithm is the approximate orientation of the sensor relative to the earth. The following block diagram of the Madgwick filter is shown in Fig. 3.

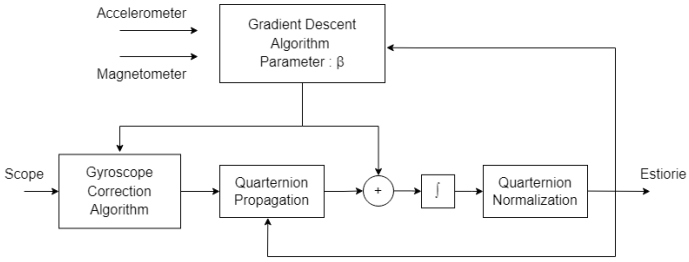

Fig 3. Madgwick filter block diagram

From Fig 3, there are two processes using the madgwick filter, the first one is using an accelerometer and magnetometer. The accelerometer and magnetometer measurements are used to correct the orientation of the gyroscope measurement error in the gyroscope correction algorithm. The gyroscope correction algorithm can also be passed by the gyroscope, this is the second way. The gyroscope correction algorithm is the combination of gyroscope measurements and correction algorithm that passed the quaternion propagation to compute the body orientation starting from the estimated of the previous step.

III. Results and Discussions

The IMU filter testing is done by comparing the results of the orientation data obtained in the Complementary and Madgwick methods. These methods' results compare the conditions of IMU sensors before and after being filtered. The data was taken in 5 conditions which are standstill, rotated to the right 90°, rotated to the left 90°, rotated up 90°, and rotated down 90° is shown in Fig. 4.

There are 3 data from each method that are being compared, namely the roll (x-axis), pitch (y-axis), and yaw (z-axis). The graph results from plot juggler on Robot Operating System. The First one is roll angle, the orange line represents pre-filtered data and the green line represents filtered data. It can be seen that, because the reference axis of rotation is on the x-axis, the graph will go up or down and be in a stable condition when the IMU is rotated to the right and to the left. The following graph results were obtained using the complementary filter method in the roll axis with the x-axis as a unit of time and the y-axis unit of degrees are shown in Fig 5.

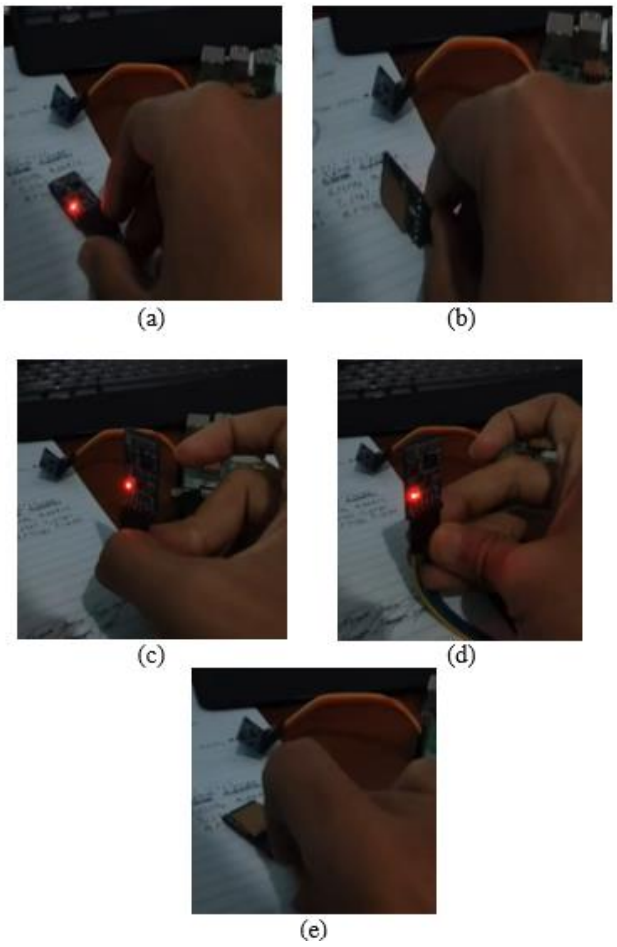

Fig 4. (a) standstill, (b) rotated to the right 90°, (c) rotated to the left 90°, (d) rotated up 90°, and (e) rotated down 90°

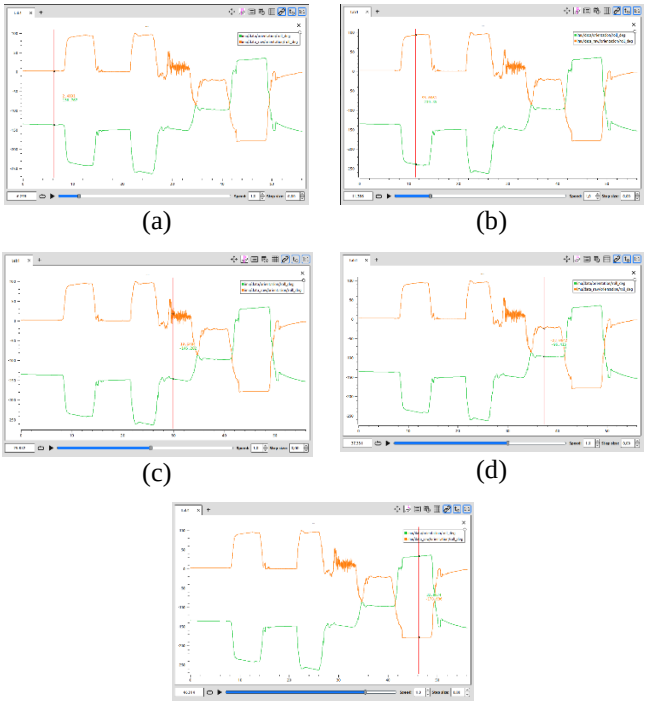

Fig 5. (a) standstill, (b) rotated right 90°, (c) rotated up 90°, (d) rotated left 90°, and (e) rotated down 90°

Second, the pitch angle, the red line represents pre-filtered data and the blue line represents filtered data. the pitch angle has a reference axis of rotation on the y-axis, so the graph will go up or down if the IMU is rotated up or down. While moving in the other direction of the axis, it will produce noise on the graph. The following graph results were obtained using the complementary filter method are shown in Fig 6. in the pitch axis.

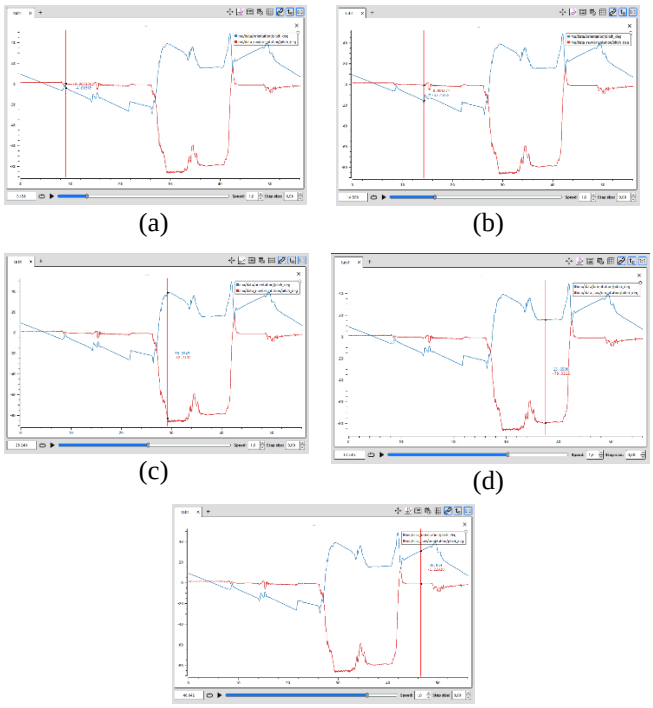

(a) (b) (c) (d) (e)

Fig 6. (a) standstill, (b) rotated right 90°, (c) rotated up 90°, (d) rotated left 90°, and (e) rotated down 90°

Third, the yaw angle, the purple line represents data pre-filtered and the pink line represents filtered data. The yaw angle has a reference axis of rotation on the z-axis, so the graph will have a change when the IMU sensor is rotated also involving a change of degrees on the z-axis. The following graph results were obtained using the complementary filter method are shown in Fig 7. in the yaw axis.

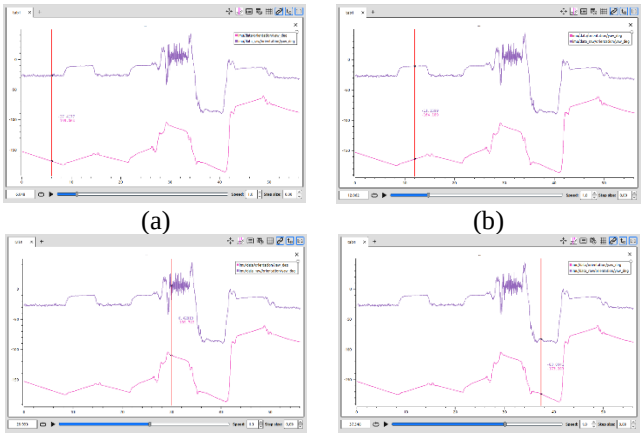

(a) (b) (c) (d)

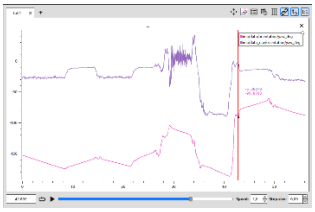

(e)

Fig 7. (a) standstill, (b) rotated right 90°, (c) rotated up 90°, (d) rotated left 90°, and (e) rotated down 90°

Meanwhile, in the Madgwick filter method, the data is taken in the same way in the same position as explained before with the 3-reference axis, roll, pitch, and yaw. The concept of the axis of rotation same as the complementary filter method. It can be seen from the results, that there is still a little noise between the filtered and unfiltered data on the three axes. It makes the resulting drift value to be quite large because there is interference from linear acceleration due to the IMU sensor that continues to move. The following graph results were obtained using the madgwick filter method with the x-axis as a unit of time and the y-axis unit of a degrees are shown in Fig 8. in the roll axis. The green line represents pre-filtered data and the red line represents filtered data.

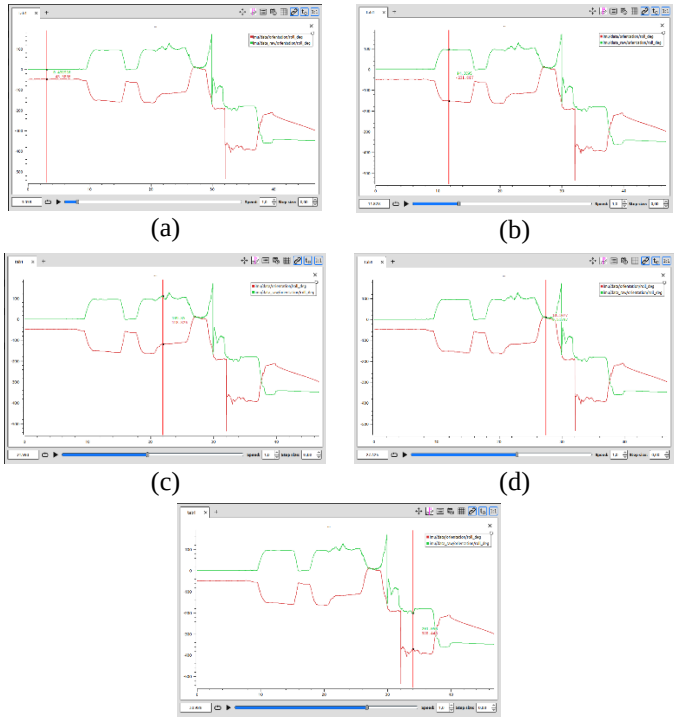

(a) (b) (c) (d) (e)

Fig 8. (a) standstill, (b) rotated right 90°, (c) rotated up 90°, (d) rotated left 90°, and (e) rotated down 90°

The following graph results were obtained using the madgwick filter method is shown in Fig 9. in the pitch axis. The red line represents pre-filtered data and the blue line represents filtered data.

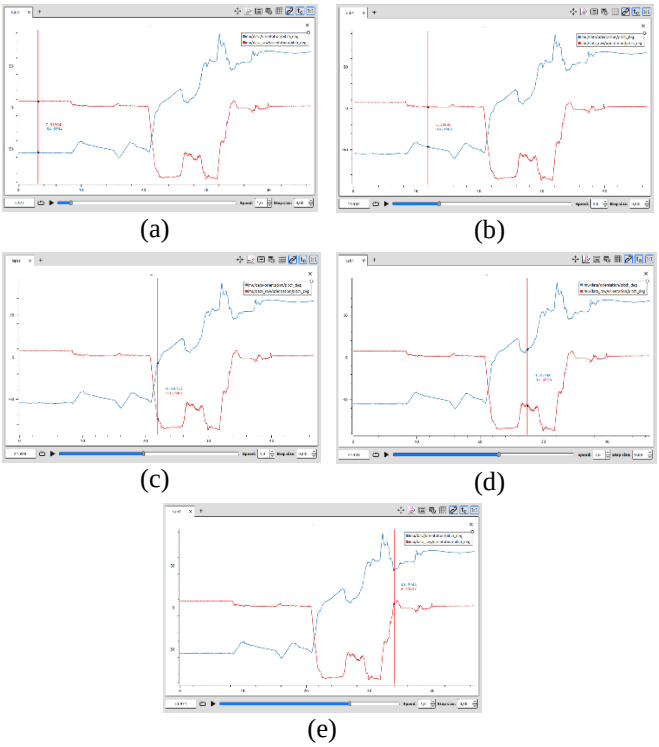

Fig 9. (a) standstill, (b) rotated right 90°, (c) rotated up 90°, (d) rotated left 90°, and (e) rotated down 90°

The following graph results were obtained using the madgwick filter method are shown in Fig 10. on the yaw axis. The green line represents pre-filtered data and the orange line represents filtered data.

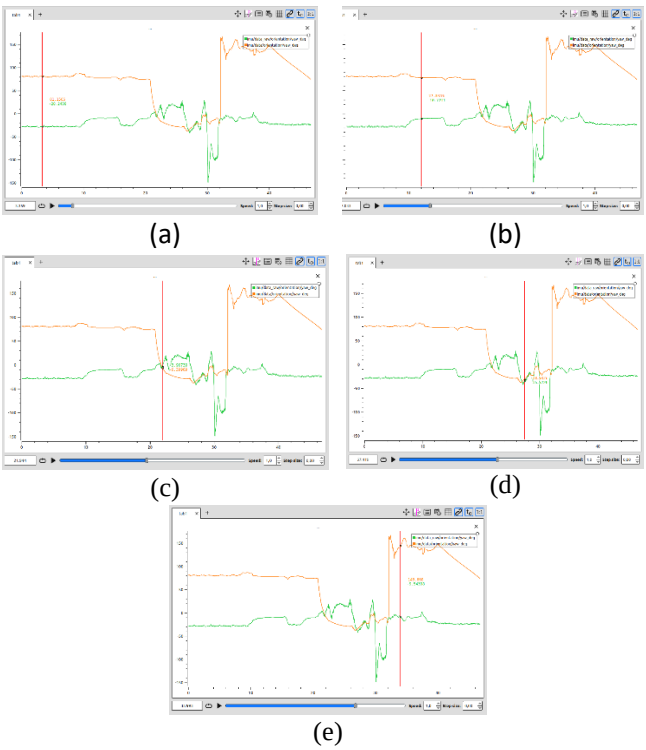

Fig 10. (a) standstill, (b) rotated right 90°, (c) rotated up 90°, (d) rotated left 90°, and (e) rotated down 90°

The data is obtained by rotating the IMU on each of the x-axis, y-axis, and z-axis so that an angle will be formed on each axis.

In the Complementary filter method, it is processed using accelerometer and gyroscope sensors. The sensor accelerometer serves to take a value in the long term (long-term) after the sensor is moved and returns to a stationary position, the data from the accelerometer sensor will be used. While the sensor is a gyroscope used to retrieve data in a short period of time (short-term) when the sensor is moved to rotate each axis.

The Madgwick method gives more results to the magnitude and direction of the gravitational field. But when measuring the magnitude and direction of the gravitational field there is a disturbance from the linear acceleration due to the IMU sensor which is constantly moving. Based on the results of the data in Fig 5. it can be seen that the noise generated when the IMU sensor is moved on three different axes is much less than that of not using the Complementary filter using the ROS algorithm. While in Fig 6. using the Madgwick method the resulting noise can still be seen clearly on the three reference axes.

IV. Conclusion

Based on the research results, it can be concluded that the results obtained using the Complementary filter method are better than the Madgwick filter which has been shown in Fig. 5-7 and Fig. 8-10. In testing the data was taken under 5 conditions, namely stationary and rotated to the right, left, up, and down by 90° each. Noise generated by the Complementary filter method can be suppressed properly using the ROS algorithm. This is because the complementary filter uses a high pass filter to remove noise on the gyroscope and a low pass filter on the accelerometer. This will cause accuracy when the robot navigates to be much better. Meanwhile, there is still noise between filtered and unfiltered data in the Madgwick method. Thus, a good filter method to use in the implementation of the covid robot is the Complementary filter, because the noise generated in the Complementary filter method can be well attenuated compared to the Madgwick filter based on the graph shown in the results and discussion.

Acknowledgment

This research is mainly funded by the “Program Penelitian Kolaborasi Indonesia (PPKI)” research program run by the Indonesian Ministry of Education, Culture, Research, and Technology and supported by Universitas Padjadjaran, Indonesia.

References

[1] K. Ruan, Z. Wu, and Q. Xu, “Smart cleaner: A new autonomous indoor disinfection robot for combating the covid-19 pandemic,” *Robotics*, vol. 10, no. 3, 2021.

[2] S. Q. Li *et al.*, “Clinical application of an intelligent oropharyngeal swab robot: Implication for the COVID-19 pandemic,” *Eur. Respir. J.*, vol. 56, no. 2, 2020.

[3] K. Jitjumnong, P. Chujai, and N. Kamata, “Robot contest for innovative development in education technology,” *Int. J. Mech. Eng. Robot. Res.*, vol. 9, no. 3, pp. 395–400, 2020.

[4] R. Syed *et al.*, “Robotic Process Automation: Contemporary themes and challenges,” *Comput. Ind.*, vol. 115, p. 103162, 2020.

[5] Y. Liu, Z. Li, H. Liu, and Z. Kan, "Skill transfer learning for autonomous robots and human–robot cooperation: A survey," *Rob. Auton. Syst.*, vol. 128, p. 103515, 2020.

[6] Z. Wang and X. Cheng, "Adaptive optimization online IMU self-calibration method for visual-inertial navigation systems," *Measurement*, vol. 180, no. April, p. 109478, 2021.

[7] S. Yu and Z. Jiang, "Design of the navigation system through the fusion of IMU and wheeled encoders," *Comput. Commun.*, vol. 160, no. April, pp. 730–737, 2020.

[8] Z. Zhe, W. Jian-bin, S. Bo, and T. Guo-feng, "Adaptive Complementary Filtering Algorithm for IMU Based on MEMS," pp. 5409–5416, 2020.

[9] S. Karam, V. Lehtola, and G. Vosselman, "Simple loop closing for continuous 6DOF LIDAR&IMU graph SLAM with planar features for indoor environments," *ISPRS J. Photogramm. Remote Sens.*, vol. 181, no. September, pp. 413–426, 2021.

[10] W. Wu *et al.*, "Low-cost wheeled robot-borne laser scanning system for indoor and outdoor 3D mapping application," *Int. Arch. Photogramm. Remote Sens. Spat. Inf. Sci. - ISPRS Arch.*, vol. 42, no. 2/W13, pp. 1155–1159, 2019.

[11] Y. Liu, N. Noguchi, and K. Ishii, "Attitude angle estimation for agricultural robot navigation based on sensor fusion with a low-cost imu", vol. 1, no. PART 1. IFAC, 2013.

[12] A. Albaghdadi and A. Ali, "An Optimized Complementary Filter For An Inertial Measurement Unit Contain MPU6050 Sensor," *Iraqi J. Electr. Electron. Eng.*, vol. 15, no. 2, pp. 71–77, 2019.

[13] D. Feng, C. Wang, C. He, Y. Zhuang, and X. G. Xia, "Kalman-Filter-Based Integration of IMU and UWB for High-Accuracy Indoor Positioning and Navigation," *IEEE Internet Things J.*, vol. 7, no. 4, pp. 3133–3146, 2020.

[14] A. Yusefi, A. Durdu, M. F. Aslan, and C. Sungur, "LSTM and filter based comparison analysis for indoor global localization in UAVs," *IEEE Access*, vol. 9, pp. 10054–10069, 2021.

[15] M. A. Hasan and M. H. Rahman, "Smart Phone Based Sensor Fusion by Using Madgwick Filter for 3D Indoor Navigation," *Wirel. Pers. Commun.*, vol. 113, no. 4, pp. 2499–2517, 2020.

[16] H. A. Hashim, M. Abouheaf, and M. A. Abido, "Geometric stochastic filter with guaranteed performance for autonomous navigation based on IMU and feature sensor fusion," *Control Eng. Pract.*, vol. 116, no. March, p. 104926, 2021.

[17] H. Rong, Y. Zhu, J. Lv, Y. Chen, C. Peng, and L. Zou, "Conditional equivalence between Extended Kalman filter and complementary filter for two-vector gyro-aided attitude determination," *Meas. J. Int. Meas. Confed.*, vol. 168, no. August 2020, p. 108428, 2021.

[18] L. Struber, S. Ledouit, O. Daniel, P. A. Barraud, and V. Nougier, "Reliability of Human Running Analysis with Low-Cost Inertial and Magnetic Sensor Arrays," *IEEE Sens. J.*, vol. 21, no. 13, pp. 15299–15307, 2021.

[19] G. Štebe, P. Krapež, J. Podobnik, and D. Kogoj, "Trajectory tracking of an oscillating movement with a low-cost IMU in geodetic surveying applications," *Meas. J. Int. Meas. Confed.*, vol. 176, 2021.

[20] C. Li, S. Wang, Y. Zhuang, and F. Yan, "Deep Sensor Fusion between 2D Laser Scanner and IMU for Mobile Robot Localization," *IEEE Sens. J.*, vol. 21, no. 6, pp. 8501–8509, 2021.

[21] F. Jamil, N. Iqbal, S. Ahmad, and D. H. Kim, "Toward accurate position estimation using learning to prediction algorithm in indoor navigation," *Sensors (Switzerland)*, vol. 20, no. 16, pp. 1–27, 2020.

[22] J. H. K. Iv, B. C. Claus, and J. C. Kinsey, "A Navigation Solution Using a MEMS IMU, Model-Based Dead-Reckoning, and One-Way-Travel-Time Acoustic Range Measurements for Autonomous Underwater Vehicles," *IEEE J. Ocean. Eng.*, vol. 44, no. 3, pp. 664–682, 2019.

[23] A. Turnip, G. M. Tampubolon, S. F. Ramadhan, A. V. Nugraha, A. Trisanto, and D. Novita, "Development of Medical Robot Covid-19 based 2D mapping LIDAR and IMU Sensors," In 2021 IEEE International Conference on Health, Instrumentation & Measurement, and Natural Sciences (InHeNce), *IEEE*, pp. 1-4, July 2021.

[24] A. Turnip, T. Hidayat, and D. E. Kusumandari," Development of brain-controlled wheelchair supported by raspicam image processing based Raspberry pi," In 2017 2nd International Conference on Automation, Cognitive Science, Optics, Micro Electro-Mechanical System, and Information Technology (ICACOMIT), *IEEE*, pp. 7-11, 2017.

[25] A. Turnip, A. I. Simbolon, M. F. Amri, and M. A. Suhendra, "Utilization of EEG-SSVEP method and ANFIS classifier for controlling electronic wheelchair," In 2015 International Conference on Technology, Informatics, Management, Engineering & Environment (TIME-E), *IEEE*, (pp. 143-146), 2015.

[26] A. Turnip, D. Soetraprawata, M. Turnip, and E. Joelianto, "EEG-based brain-controlled wheelchair with four different stimuli frequencies," *Internetworking Indonesia Journal*, 8(1), 65-69, 2016.

[27] E. Joelianto, A. Turnip, and A. Widyotriatmo, "Cyber Physical, Computer and Automation System," *Springer Singapore*, 2021.